Electron Emission from Metal Surfaces by Ultrashort Pulses: Determination of the Carrier-Envelope Phase

C. Lemell,[1,*] X.-M. Tong,[2] F. Krausz,[3] and J. Burgdörfer[1]

[1]*Institute for Theoretical Physics, Vienna University of Technology, Wiedner Hauptstraße 8-10, A-1040 Vienna, Austria*
[2]*Department of Physics, 116 Cardwell Hall, Kansas State University, Manhatten, Kansas 66506*
[3]*Photonics Institute, Vienna University of Technology, Gusshausstraße 27, A-1040 Wien, Austria*

(Received 22 August 2002; published 21 February 2003)

The phase φ of the field oscillations with respect to the peak of a laser pulse influences the light field evolution as the pulse length becomes comparable to the wave cycle and, hence, affects the interaction of intense few-cycle pulses with matter. We theoretically investigate photoelectron emission induced by an intense, few-cycle laser pulse from a metal surface (jellium) within the framework of time-dependent density functional theory and find a pronounced φ dependence of the photocurrent. Our results reveal a promising route to measuring φ of few-cycle light pulses ($\tau < 6$ fs at $\lambda = 0.8$ μm) at moderate intensity levels ($I_p \approx 10^{12}$ W/cm^2) using a solid-state device.

DOI: 10.1103/PhysRevLett.90.076403 PACS numbers: 71.15.Mb, 73.50.Fq, 79.20.Ds, 79.60.–i

Recent progress in ultrashort-pulse laser technology has resulted in the generation of intense optical pulses comprising merely one and a half wave cycles T_0 within the full width at half maximum τ of their temporal intensity profile ($\tau = 4$ fs at a wavelength of 780 nm, where $T_0 = 2.6$ fs) [1]. Intense few-cycle, sub-10-fs light pulses are now available at several wavelengths [2] and are about to open up a number of applications ranging from nanometer-scale materials processing [3] to the generation of coherent soft-x-ray radiation for biological microscopy [4].

With τ becoming comparable to T_0, the temporal evolution of the electric and magnetic fields of a few-cycle light pulse and, hence, all nonlinear processes driven by these fields become increasingly affected by the carrier-envelope (or absolute) phase φ. A prominent example is the emergence of isolated subfemtosecond x-ray pulses from few-cycle-driven high-harmonic generation [5]. The reproducible generation of these pulses, which is of crucial importance for attosecond innershell spectroscopy, relies on stabilization and precise control of φ. Whereas the pulse-to-pulse change of φ can now be precisely controlled at the output of mode-locked oscillators [6] and can be measured even in amplified pulses [7], all attempts to determine the value of φ in a pulse failed thus far. Photoionization of atoms in the strong-field regime (referred to as optical-field or quasistatic ionization) has been identified as a promising process for providing a physical measurable sensitive to φ [8–10] together with predictions of an increased phase contrast already at moderate laser intensities ($I_p \approx 10^{12}$ W/cm^2, [11]). Detectable phase effects, however, could be observed only for circularly polarized light thus far [12]. Because of symmetry breaking along the surface normal, photoemission from metals is expected to be another experimentally accessible phase sensitive measurable. Estimates for the strong-field regime based on quasistatic ionization rates supported this expectation [13], but the feasibility of experimental implementation remained questionable because of the high peak intensities required to enter the quasistatic regime of photoionization.

In this Letter, we present the first fully time-dependent treatment of this process. Our numerical study corroborates previous estimates [13] in the quasistatic regime but yields unexpected (and very promising) results at lower intensity levels, where the ionization process becomes nonadiabatic (multiphoton regime). In this regime characterized by a Keldysh parameter γ [14] significantly larger than 1, we obtain a qualitatively different and *strongly enhanced* dependence of the integrated photocurrent on φ as compared to that characteristic of the quasistatic regime. The time-integrated photocurrent is predicted to vary by some 25% for a 5-fs pulse carried at a wavelength of 790 nm at intensity levels far below the damage threshold, opening the door to the measurement of φ of a linearly polarized few-cycle laser pulse.

We employ the time-dependent density functional theory (e.g., [15,16] and references therein) to determine the electronic evolution of a metal surface modeled by a jellium surface under the influence of a few-cycle laser pulse (pulse durations $\tau = 4$–10 fs at $\lambda = 790$ nm) with peak intensities I_p between 5.6×10^{11} W/cm^2 and 1.7×10^{14} W/cm^2. The extended size of such a system poses a formidable challenge for a description of a time-dependent many-body system. Typical laser spot sizes in the experiment have a diameter of about 3 μm ($\sim$60.000 a.u.), which, at typical metallic densities, implies $\gtrsim 10^8$ conduction electrons subject to the electric pulse in the surface layer. Moreover, during the pulse duration of $\tau \approx 10$ fs ($\approx$400 a.u.), electrons can travel many hundreds of atomic units into the bulk requiring a large slab depth. Therefore, drastic simplifications are called for to reduce the system to a manageable size. We assume in the following that the linear polarization is oriented along the surface normal corresponding

to approximately grazing incidence of the laser pulse and an infinitely large spot size. Under these simplifying assumptions, the translational symmetry of the Hamiltonian in the plane of the surface is preserved in the presence of the pulse. Consequently, the separability of the ground-state Kohn-Sham orbitals

$$\psi_{l,\vec{k}}(\vec{r}) = \phi_l(z)\exp(i\vec{k}\vec{R})/\sqrt{2}\pi, \quad (1)$$

where z denotes the coordinate along the surface normal and $\vec{R}$ the vector in the surface plane, into two-dimensional plane waves, and a discrete orbital ϕ_l for the degree of freedom along the surface normal remains valid throughout the propagation in the strong pulse. The orbitals are solutions of the time-dependent Kohn-Sham equations:

$$i\partial_t\psi_{l,\vec{k}}(\vec{r},t) = (H_0 + \delta V_{\text{eff}}[n(t)] - zF(t))\,\psi_{l,\vec{k}}(\vec{r},t). \quad (2)$$

In Eq. (2), H_0 is the effective Kohn-Sham Hamiltonian for the ground state of the jellium surface; δV_{eff} represents the change in the effective potential due to the induced time-dependent density fluctuations. The last term describes the coupling to the laser pulse $F(t)$. The temporal profile is written as

$$F(t) = F_{\text{env}}(t)\cos(\omega t + \varphi), \quad (3)$$

where $F_{\text{env}}(t)$ is the envelope function chosen to be a Gaussian, $F_0\exp(-t^2/2\tau^2)$, with a FWHM of τ between 4 and 10 fs. ω is the carrier frequency and φ the carrier-envelope phase.

Following Eguiluz *et al.* [17,18], the jellium surface is represented in terms of a slab: A jellium slab of thickness d (all results in this paper are for $d = 48r_s$, r_s the Wigner-Seitz radius) and with constant positive background density n_+ is situated inside a hard-walled box of width L. n_+ is uniquely determined by the only free parameter in a jellium description, r_s characterizing the uniform bulk electron density of the metal. The distance $a = (L - d)/2$ between the jellium surface and the confining wall must be large compared to the quiver amplitude of a free electron in an electromagnetic field, $a \ll a_q = F/\omega^2$, in order to prevent unphysical distortions of the wave packet due to boundary effects. In line with experiments, we choose as carrier frequency $\omega = 0.057$ a.u. corresponding to the wavelength of $\lambda = 790$ nm. The orbitals $\phi_l(z)$ representing subbands of the initial ground state are solutions of the stationary Kohn-Sham equations. The exchange-correlation potential $V_{\text{xc}}(z)$ entering the effective one-particle potential $V_{\text{eff}}[n(z)]$ is calculated in the local density approximation (LDA). The LDA is known to lead to an exponential rather than to a correct $-1/4z$ dependence of the image potential far from the surface [19–21]. We use this approximation for the sake of its simplicity and the reduction of computing time. However, a $-1/4z$ image tail can be included as an external potential on a phenomenological level. This allows one to test for the sensitivity of φ to the asymptotic limit of the exchange-correlation potential. Along similar lines, in order to test the dependence on the work function, we have changed the work function of the jellium at fixed r_s by adding an additional potential that is constant inside the slab and decays exponentially towards the vacuum with a characteristic length r_s, thereby introducing a second adjustable parameter to the jellium model. This modified jellium allows one to probe the W and r_s dependence of the photoemission independently. Clearly, switching off this additional potential leads to the standard jellium model where W is uniquely determined by r_s.

For the determination of $\phi_l(z)$ and of ε_l, we apply the Fourier grid Hamiltonian method [22] with a grid spacing $\Delta z = 0.2r_s$ equivalent to a grid size in momentum space of $\Delta k = 2\pi/N\Delta z \approx 0.0627/r_s$. The solution of the Kohn-Sham equation is thus reduced to the eigenvalue problem of the Hamiltonian matrix H_{ij} of dimension of the order of $N \times N$ with $N \approx 500$. Time propagation of the Kohn-Sham orbitals was performed by a second-order split-operator method (see, e.g., [23] and references therein). In contrast to the more commonly used split of the Hamiltonian H into kinetic and potential terms, our algorithm is based on the splitting of H into the time independent ground-state Hamiltonian $H_0(z)$ and a time-dependent potential $\tilde{V}(z,t)$, which includes the external perturbation (the laser field) and changes $\delta V_{\text{eff}}(z) = V_{\text{eff}}(z,t) - V_{\text{eff},0}$ of the effective potential relative to that of the ground state. Care must be taken of unphysical reflections due to the boundaries of the finite-size model system. Two classes of reflections have to be considered. Reflections at the hard wall box are damped by "masking" functions, i.e., absorbing boundaries or, equivalently, optical potentials [24,25]. The mask on the vacuum side serves in the present case in addition as a microscopic detector for the photocurrent of ionized electrons. A different type of unphysical reflection occurs due to the finite thickness of the slab: Density fluctuations generated at the surface propagate through the slab and are reflected at the "back side" of the slab. Since the round-trip time of the fluctuation through the slab is comparable to the duration of the pulse (~ 500 a.u.), they can distort the electronic evolution at the "front" surface, unlike for the semi-infinite solid. These density fluctuations have also been damped out by an optical-potential barrier close to the back side of the slab.

Figure 1 shows the integrated emitted charge per laser pulse as a function of the maximum field strength F_0, for two different work functions W corresponding to different r_s values and the duration of the pulse of $\tau = 10$ fs. For moderate field strength ($\gamma > 1$), the integrated intensity for photoemission, I_{PE}, closely follows a power law with the exponent of F_0 being almost a linear function of the work function W of the metal (see inset in Fig. 1). Keeping ω constant but varying W reveals a linear

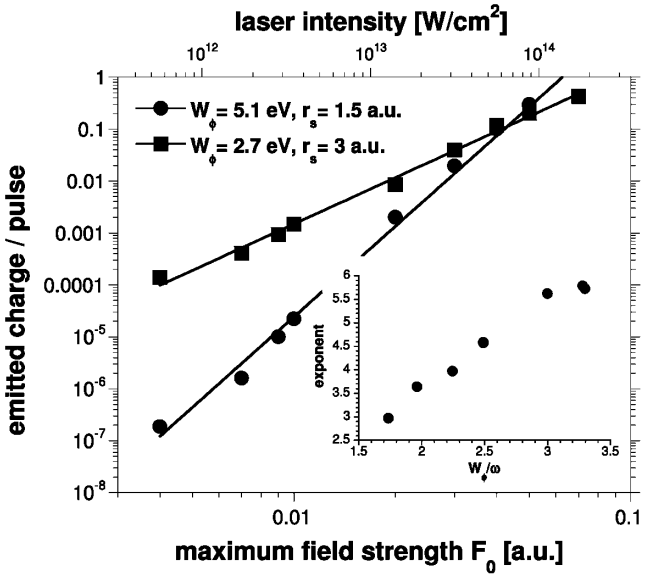

FIG. 1. Dependence of the photoemission on maximum field strength F_0 of the laser pulse for modified jellia with different density ($r_s = 1.5$, 3) and work function ($W = 5.1$ eV, 2.7 eV). Inset: exponent x of $I_{\mathrm{PE}} \propto F_0^x$ as a function of W/ω.

dependence of the exponent on the ratio W/ω. Such a dependence is characteristic of the multiphoton regime (see [1]). By keeping W fixed while varying r_s (modified jellium model), we find only a weak dependence on the density, or, equivalently, the Fermi energy.

Although ultrashort laser pulses have the decisive advantage of a small energy deposition even for high peak intensities I_p, the damage threshold is reached at I_p of the order of a few 10^{13} W/cm^2. Nevertheless, we have also calculated photoemission for larger I_p in order to investigate the transition from the multiphoton to the strong-field regime defined by a Keldysh parameter for solids $\gamma = \omega\sqrt{W}/F_0 < 1$ [14]. In this regime, the Keldysh formula predicts a slight deviation from a pure power law $I_{PE} \propto F_0^x$, which is barely noticeable for $F_0 \gtrsim 0.03$.

By contrast, γ is found to have a much greater influence on the time-resolved emission characteristics. In Fig. 2, we show results for the time-resolved photoemission from a jellium surface with $r_s = 3$ ($W = 3.48$ eV) for a pulse duration of $\tau = 5$ fs and for (a) γ smaller and (b) γ larger than 1. For both the strong-field case ($\gamma < 1$) and the weak-field case ($\gamma > 1$), we show the time-resolved emission for different carrier-envelope phases $\varphi = 0$ and π. In the strong-field case, the electron emission closely tracks the half cycles of the pulse that lower the surface barrier potential (in analogy to the atomic case in the following referred to as the "downhill" half cycle), while in the multiphoton case ($\gamma > 1$) almost no trace of the carrier oscillation can be found. The important point to be noted is that the preferred direction of the surface normal breaks the inversion symmetry of the Hamiltonian with respect to the field ($\vec{F} \rightarrow -\vec{F}$).

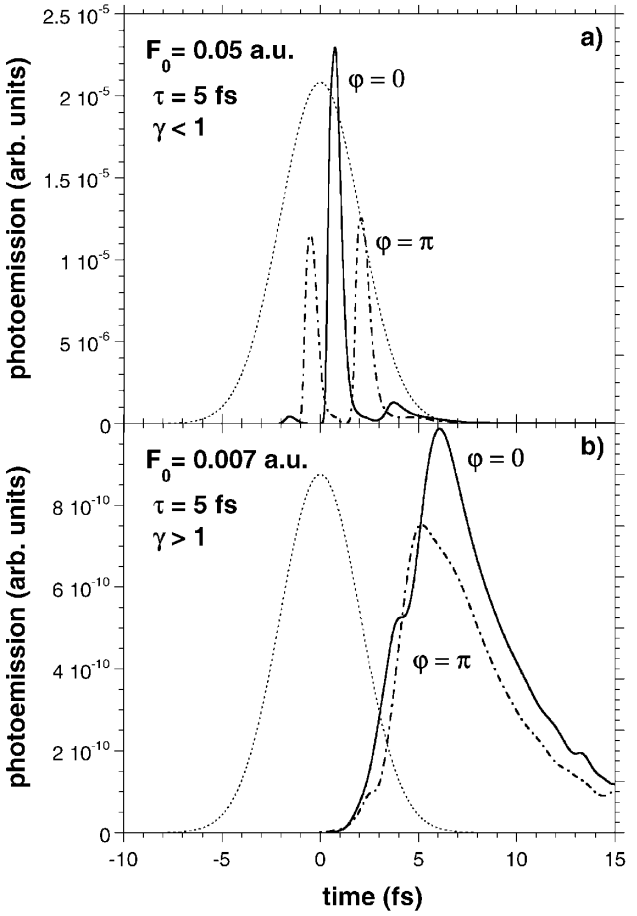

FIG. 2. Time-resolved electron emission for different carrier-envelope phase φ and peak field strength of (a) $F_0 = 0.05$ ($\gamma < 1$) and (b) $F_0 = 0.007$ ($\gamma > 1$). Dotted lines indicate the envelope function of the laser pulse with $\tau = 5$ fs. Note the difference in scale in plots (a) and (b).

Unlike free atoms, the "uphill" and downhill half cycles contribute very differently to the emission, resulting in a φ sensitivity of the photocurrent. The time delay between the maxima of the oscillations and the emission peaks is due to the finite travel time from the surface to the "detector," i.e., the absorbing wall. The mean energy of the electrons calculated from the distance of the detector from the surface and the time delay between the field maximum and the detection [≈ 1.3 eV, Fig. 2(b)] is almost equal to 3 times the photon energy reduced by the work function of the jellium slab (≈ 1.17 eV). In agreement with these findings, the expansion of our wave functions into Kohn-Sham orbitals of the systems features distinct peaks at coefficients corresponding to energies $E_F + n \cdot \hbar\omega$ corresponding to multiphoton excitation for $\gamma > 1$. The strong φ dependence can be visualized in the limit of short τ such that effectively only one half cycle interacts with the surface. While a pulse in the downhill direction (i.e., $\varphi = 0$) leads to direct field emission, the main effect of the pulse in the

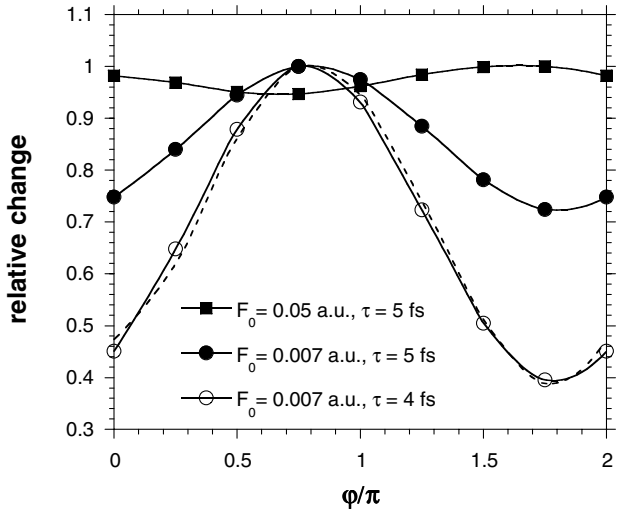

FIG. 3. Variation of the time-integrated photoemission with the absolute phase and the maximum field strength F_0 of the laser pulse. Solid symbols: Same laser parameters as in Fig. 2; open symbols: $F_0 = 0.007$ a.u., $\tau = 4$ fs. The dashed line shows the photoemission when a long range image tail $(-1/4z)$ is added.

uphill direction ($\varphi = \pi$) is a density fluctuation traveling through the metal reducing the charge emission by orders of magnitude. The observed strong φ dependence (Fig. 2) clearly indicates that for few-cycle pulses φ plays a decisive role in the electronic response of the surface. This observation carries over to the integrated emission current. In Fig. 3, we show the phase dependence of the total emitted charge per pulse for the same laser parameters as in Figs. 2(a) and 2(b). The modulation with φ depends parametrically on the field strength F_0 as well as on the pulse duration τ. The maximum of the electron emission as a function of φ shifts as F_0 undergoes a transition from the strong-field regime ($\gamma < 1$) to the multiphoton regime ($\gamma > 1$). Its position remains, however, stable for different values of F_0 within the multiphoton regime. It also displays little variation when the image potential is added which is due to the fact that the additional $-1/z$ potential seen by the ionized electron overshadows the image tail. Moreover, the variation and, consequently, the phase contrast increases with decreasing field strength. This observation is crucial for the feasibility of measurements of the carrier-envelope phase. Variations in F_0 across the laser spot do not average out the modulation as a function of φ as long as the maximum F_0 at the center of the spot is already in the regime $\gamma > 1$. Further reduction in pulse duration ($\tau = 4$ fs in Fig. 3) enhances the variation with φ, i.e., the phase contrast.

In summary, we have shown that the photocurrent from a jellium surface irradiated with ultrashort laser pulses strongly depends on the "absolute" (or carrier-envelope) phase of the laser pulse. The strong variation is, in part, due to the fact that the surface breaks the inversion symmetry ($\varphi \rightarrow \varphi + \pi$) for laser-matter interaction. Even if one considers a reduction in contrast for oblique incidence (not treated in the present calculation), we expect that measurement of photocurrents for metal surfaces already at moderate laser intensities ($I_p \approx 10^{12}$ W/cm^2, $\gamma \approx 2$–3) opens a promising new pathway for determining and controlling the absolute phase of ultrashort laser pulses.

This work has been supported by the special research program FWF-SFB016 "ADLIS."

*Electronic address: lemell@concord.itp.tuwien.ac.at

[1] T. Brabec and F. Krausz, Rev. Mod. Phys. **72**, 545 (2000).
[2] G. Steinmeyer *et al.*, Science **286**, 1507 (1999).
[3] M. Lenzner *et al.*, Phys. Rev. Lett. **80**, 4076 (1998).
[4] Ch. Spielmann *et al.*, Science **278**, 661 (1997).
[5] M. Hentschel *et al.*, Nature (London) **414**, 509 (2001).
[6] D. J. Jones *et al.*, Science **288**, 635 (2000); A. Apolonski *et al.*, Phys. Rev. Lett. **85**, 740 (2000); U. Morgner *et al.*, Phys. Rev. Lett. **86**, 5462 (2001); R. Holzwarth *et al.*, Phys. Rev. Lett. **85**, 2264 (2000); H. R. Telle *et al.*, Appl. Phys. B **69**, 327 (1999); S. T. Cundiff, J. Phys. D **35**, R43 (2002).
[7] M. Kakehata *et al.*, Opt. Lett. **26**, 1436 (2001); M. Mehendale *et al.*, Opt. Lett. **25**, 1672 (2000).
[8] I. P. Christov, Opt. Lett. **24**, 1425 (1999).
[9] P. Dietrich *et al.*, Opt. Lett. **25**, 16 (2000).
[10] S. Chelkowski and A. D. Bandrauk, Phys. Rev. A **65**, 061802 (2002).
[11] G. L. Yudin and M. Yu. Ivanov, Phys. Rev. A **64**, 013409 (2001).
[12] G. G. Paulus *et al.*, Nature (London) **414**, 182 (2001).
[13] A. Poppe *et al.*, in *Trends in Optics and Photonics*, OSA Proceedings Series 28 (Optical Society of America, Washington, DC, 1999), p. 31.
[14] L. V. Keldysh, Sov. Phys. JETP **20**, 1307 (1965).
[15] K. Burke and E. K. U. Gross, in *Density Functionals: Theory and Applications*, edited by D. Joubert (Springer-Verlag, Berlin, 1998).
[16] N. T. Maitra *et al.*, in *Reviews in Modern Quantum Chemistry: A Celebration of the Contributions of R. G. Parr*, edited by K. D. Sen (World Scientific, Singapore, 2001).
[17] A. G. Eguiluz *et al.*, Phys. Rev. B **30**, 5449 (1984).
[18] A. G. Eguiluz, Phys. Rev. Lett. **51**, 1907 (1983).
[19] P. A. Serena *et al.*, Phys. Rev. B **34**, 6767 (1986).
[20] E. Chacón and P. Tarazona, Phys. Rev. B **37**, 4020 (1988).
[21] A. G. Eguiluz *et al.*, Phys. Rev. Lett. **68**, 1359 (1992).
[22] C. C. Marston and G. G. Balint-Kurti, J. Chem. Phys. **91**, 3571 (1989).
[23] X.-M. Tong and S. I. Chu, Chem. Phys. **217**, 119 (1997).
[24] D. R. Schultz *et al.*, Phys. Rev. A **50**, 1348 (1994).
[25] S. Yoshida *et al.*, Phys. Rev. A **60**, 1113 (1999).